Bulletin of Geophysics and Oceanography Vol. XX, n. X, pp. XXX-XXX; Xxxxx 20xx
DOI 10.4430/bgo00466

High-resolution modelling of a shallow marginal sea to assess the potential of energy production from marine currents: the northern Adriatic Sea case study

F. Giordano[1,2], S. Querin[1], M. Reini[2] and S. Salon[1]

[1] *National Institute of Oceanography and Applied Geophysics - OGS, Trieste, Italy*
[2] *University of Trieste, Trieste, Italy*

(Received: 17 May 2023; accepted: 30 May 2024; published online: 13 September 2024)

ABSTRACT The Northern Adriatic Sea Reanalysis and Forecasting (NARF) system is a high-resolution (1/128°) modelling system designed to perform multi-purpose simulations (e.g. from decadal to operational temporal scales) of the oceanographic properties of the northern Adriatic Sea. Validation and quality assessment of horizontal current fields have been carried out for the 2006-2017 time period by comparing model outputs both with available observations and larger scale Copernicus Marine Service (CMS) reanalyses, showing better agreement with the experimental data, and a reduction of the average bias against observations compared to the lower resolution CMS products. In addition, NARF current speed was encountered to be generally more intense, with an overall increase of up to 50% compared to the lower resolution model. This data set was used to assess the energy potential of marine currents in the northern Adriatic. By analysing the statistics of the velocity fields, five areas, where the currents are more intense, were identified. However, none of the selected sites proved to be suitable for large-scale energy generation. Nevertheless, due to the better description of basin hydrodynamics, a drastic increase in the estimated power flux was observed when switching from lower resolution CMS to NARF reanalyses. This work emphasises the importance of high-resolution models in the field of renewable energy feasibility analysis, planning and design.

Key words: marine renewable energy, physical oceanography, coastal areas, Adriatic Sea, hydrodynamic modelling.

1. Introduction

Marine Renewable Energy (MRE) production still lags behind other renewable energy sources such as wind and solar power, which are technologies mature enough to be commercially employed on a large scale.

However, there is an increasing interest in MRE solutions due to the sheer volume of energy contained in the ocean: on a global scale, the various ocean energy sources have been estimated to be thousands (from marine currents and salinity gradients) or even tens of thousands (from wave motion and thermal gradients) of TWh per year (Brito-Melo *et al.*, 2007).

Such an interest has been expressed through the strategies, issued by the European Commission in the framework of Sustainable Blue Economy, which are driven by the necessity to face climate change, thus abandoning fossil fuels as the main mean of energy supply. This would

also allow for less dependence on foreign oil and gas exports, instead providing a higher share of power from the many seas of Europe: more than a hundred sites have been identified as suitable for tidal current energy production along the shores of the continent (European Commission, 1996). While many of these sites are located in the Atlantic Ocean, the Mediterranean Sea has also received interest for marine energy production. Nikolaidis *et al.* (2019) reviewed the Mediterranean Sea's potential for what is known as blue energy, a broader definition including any energy source deriving from the sea, such as offshore wind power and marine biomass. Good exploitability in many regions was found, highlighting the potential for marine currents power in straits, e.g. in the Aegean Sea and in the straits of Messina and Gibraltar. For these two straits, more detailed studies were also carried out, both to assess the energy potential with high-resolution models (Calero Quesada *et al.*, 2014) and to design devices such as turbines (Coiro *et al.*, 2018; Hazim *et al.*, 2021), showing high energy fluxes exploitable, with tens to hundreds of kilowatts of power generation capabilities. Conversely, marginal seas have remained largely not studied. One such example is the Adriatic Sea where, despite its active ocean dynamics and strong variability, only a very few studies tackled the feasibility of energy production from marine currents in the area (Hadžić *et al.*, 2014).

In this paper, the potential of renewable energy generation in the northern Adriatic Sea (NAS) is assessed by analysing the output of a high-resolution hydrodynamic model. In Section 2 we give an outline of the NAS circulation. In Section 3 we describe the numerical models considered (and compared) and the experimental data available. In Section 4 we validate the results and assess the potential of energy production. In Section 5 we discuss the feasibility of power generation and the possible applications. The conclusions and future perspectives are outlined in Section 6.

2. Study site: the northern Adriatic Sea

The Adriatic Sea is a marginal sea of the Mediterranean, extending north-westwards for about 800 km in length and 200 km in width between the Italian and Balkan peninsulas (Gačić *et al.*, 2001).

The mean basin-scale circulation is cyclonic (Poulain and Cushman-Roisin, 2001). Warmer and saltier waters enter through the Strait of Otranto to the south flowing in the weak Eastern Adriatic Current (EAC) along the eastern, more rugged shoreline, while colder waters are advected into the Western Adriatic Current (WAC) flowing out along the western, smoother coasts (Poulain and Cushman-Roisin, 2001). Three sub-basin circulation patterns (southern, middle, and northern Adriatic) are induced mainly by bathymetric constraints (Poulain and Cushman-Roisin, 2001), while other smaller-scale recirculations can be generated by meteorological forcing (e.g. Kuzmić *et al.*, 2006).

The NAS is characterised by a shallow bathymetry, averaging around 40 m in depth (Gačić *et al.*, 2001), and by the concurrence of many forcings (Poulain and Raicich, 2001). In particular, the atmosphere exchanges both momentum and heat with the NAS.

Winds, mainly the south-easterly Sirocco and east-north-easterly Bora, affect the surface currents (Poulain and Raicich, 2001). In particular, the Bora may characterise the dynamics, affecting the velocity across much of the water column (Ličer *et al.*, 2016) and creating circulation patterns in the northern section of the NAS (Kuzmić *et al.*, 2006).

The sea also loses heat, with an average rate of 20 W/m², to the atmosphere, with peaks up to 1,000 W/m² during intense Bora events, which facilitates surface cooling and evaporation

(Poulain and Raicich, 2001). This process also causes the formation and advection, as a bottom density current, of the North Adriatic Dense Water, one of the densest water masses of the whole Mediterranean, contributing to the oxygenation of its deepest layers (Poulain and Cushman-Roisin, 2001).

Freshwater inputs also play an important role: around 20% of the total Mediterranean river runoff is conveyed into the NAS, mainly due to the presence of the Po River (Poulain and Raicich, 2001). These strong freshwater inputs clearly affect the dynamics, providing colder, fresher, and nutrient-rich waters to the basin (Poulain and Raicich, 2001).

Beyond the spatial variability, a seasonal cycle can be clearly observed in the circulation intensity (Poulain, 2001), for example in the WAC, which strengthens during autumn and weakens in the spring and summer months.

Other transient phenomena, such as Bora events, can cause abrupt changes in the circulation, enriching and strengthening the NAS dynamical features. The typical jet-like pattern of the Bora wind field, related to the orographic gaps where these cold air masses are channelled, causes the formation of surface shear stress and in turn triggers basin-scale structures such as the double-gyre circulation described in Kuzmić *et al.* (2006).

Several experimental and modelling studies covered almost all the aspects of the Adriatic Sea oceanography. Reference climatologies have been obtained from measurements [for example in Solidoro *et al.* (2009) and Lipizer *et al.* (2014)], capitalising on the vast quantity of observational records in the Adriatic Sea. As a 'laboratory' for coastal dynamics (Umgiesser *et al.*, 2022), many models have been implemented in the Adriatic region. Some were used to perform reanalyses, thus describing physical and biogeochemical dynamics on multi-decadal timescales (e.g. Silvestri *et al.*, 2020). Others focused on regional studies, both hindcasts, such as the one by Pranić *et al.* (2021) investigating the effect of high resolution in dynamical and thermohaline characteristics like the formation and fate of northern Adriatic dense water, and projections into global warming scenarios (Denamiel *et al.*, 2020). High-resolution simulations are also employed for operational models, to assess and predict potential hazards, from storm surges (Ferrarin *et al.*, 2020) to microbial contamination (Bruschi *et al.*, 2021), and to produce short-term forecasts of the physical and biogeochemical state of the sea (https://medeaf.ogs.it/adriatic).

3. Materials and methods

This study is based on numerical simulations and experimental data: the former are provided by the Northern Adriatic Sea Reanalysis and Forecasting (NARF) model (Section 3.1.) and the Copernicus system (Section 3.2.), the latter are obtained from acoustic Doppler current profilers (ADCPs) and satellite data (Section 3.3.). The NARF data set is, then, employed to estimate power fluxes via the Betz Law (Section 3.4.).

3.1. The Northern Adriatic Sea Reanalysis and Forecasting system

The NARF is a modelling system developed at OGS in the framework of several national and European projects for marine environmental monitoring in the NAS [e.g. CADEAU project: Silvestri *et al.* (2020), Bruschi *et al.* (2021)], capitalising on the results and consolidated expertise obtained in previous research activities. The modelling system was firstly implemented for physical purposes: from the description of general circulation to the analysis of dense water formation (Querin *et al.*, 2013) and bottom dynamics (Querin *et al.*, 2016). Later, the system

was expanded to include biogeochemical cycles (Cossarini *et al*., 2015, 2017) and to provide boundary conditions for local, finer resolution, nested simulations, such as the ones performed by Querin *et al*. (2021) for the Gulf of Trieste and by Petronio *et al*. (2013) for the Muggia Bay (the industrial harbour of Trieste).

The NARF is based on the coupled MITgcm and BFM models: while the latter model describes biogeochemical interactions (Vichi *et al.*, 2015), the former is a hydrodynamical model that can be operated in a non-hydrostatic configuration (Adcroft *et al.*, 2022). The system solves the motion equations on a regular grid composed of 300×494 horizontal cells in latitude and longitude, respectively, corresponding to a horizontal resolution of 1/128° (approximately 800×600 m^2), and 27 unequally spaced vertical levels (Silvestri *et al.*, 2020) to cover the spatial domain shown in Fig. 1.

In the framework of the CADEAU project, the modelling system has been used to produce a simulation of the NAS circulation covering a period of 12 years (from 2006 to 2017), with an integration time step of 200 s and daily averaged output data (Silvestri *et al.*, 2020).

The NARF takes into account surface atmospheric forcing provided by two different models: the 12-kilometer resolution RegCM4 model for the 2006-2012 time period (Giorgi *et al.*, 2012) and the 2.8-kilometer resolution COSMO-I2 model for the 2013-2017 time period[1]. Freshwater inputs are included and consider the 19 main rivers flowing into the NAS. For three of these (Po, Isonzo/Soča, and Timavo), measured daily flow rates are available while the rest have been described by seasonally modulated climatological values (Querin *et al.*, 2013). Both the southern boundary and the initial conditions have been provided by the Copernicus Marine Service (CMS) Mediterranean reanalysis products. At the southern boundary, a nudging scheme has been implemented to gradually relax the state of the model to the imposed conditions.

The model does not resolve surface gravity waves and it neglects tides: the latter aspect, in particular, must be taken into account when evaluating the results in terms of energy production, will be discussed in Section 5.

Ultimately, the NARF employs data assimilation schemes for satellite sea surface temperature, as well as other biogeochemical variables (e.g. nutrients) obtained from in-situ measurements (Silvestri *et al.*, 2020).

3.2. Copernicus Marine Service reanalysis

The CMS Mediterranean Sea physics reanalysis (Escudier *et al.*, 2020, 2021) simulates the dynamics of the whole basin at a horizontal resolution of 1/24° (about 4 km) and with 141 unequally spaced vertical levels, spanning a period from 1987 to present, therefore, enabling the comparison between the two modelling systems that overlap in time.

CMS reanalysis is based on the Nucleus for European Modelling of the Ocean v3.6 hydrodynamical model, it assimilates temperature and salinity vertical profiles and satellite sea level anomaly along track data via a variational scheme (OceanVAR), and employs the ERA5 atmospheric model to force ocean dynamics. Runoff is considered for 39 rivers, 10 of which flow into the NAS.

3.3. Observational data

In the analysed time period, the available observations were obtained from two sources.

Moored acoustic Doppler current profilers (ADCPs) (whose locations are shown in Fig. 1b)

[1] https://www.arpae.it/it/temi-ambientali/meteo/scopri-di-piu/il-modello-meteorologico-cosmo-lami

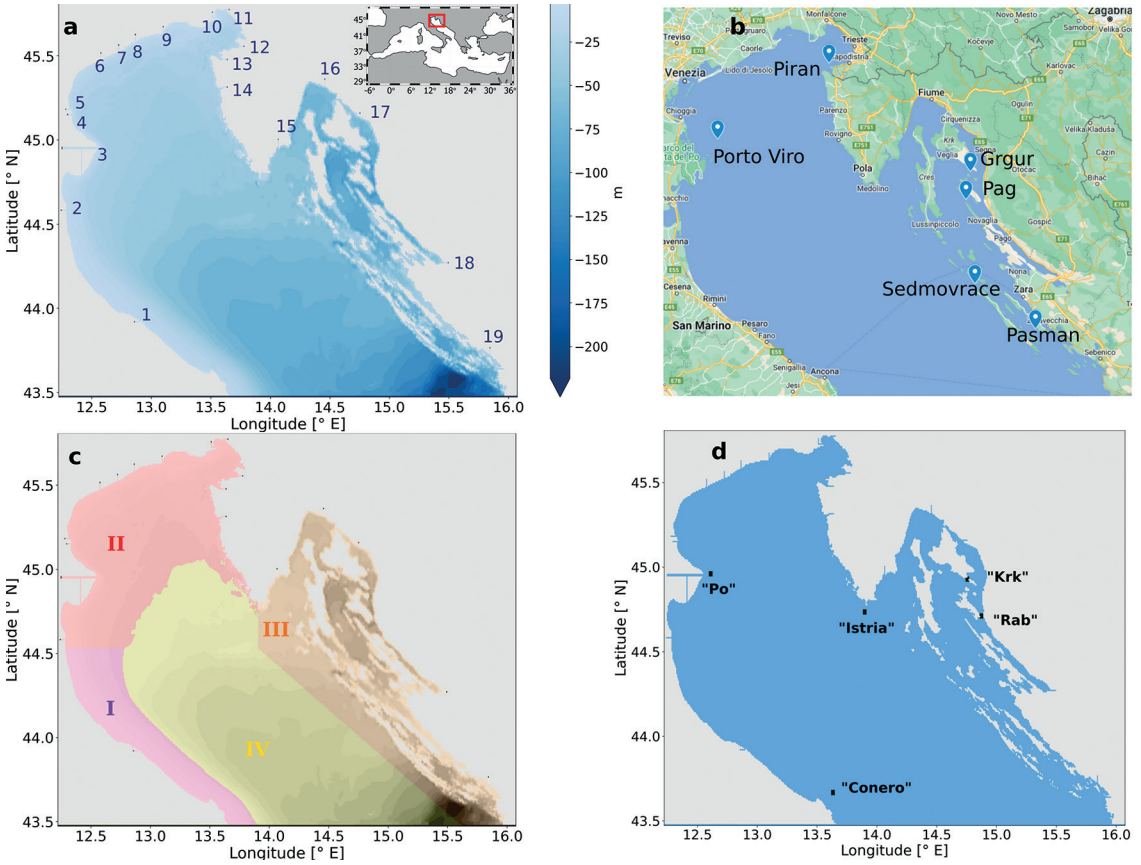

Fig. 1 - a) Location and bathymetry of the computational domain and 19 rivers considered: 1) Foglia, 2) Reno and Lamone, 3) Po, 4) Adige, 5) Brenta, 6) Sile, 7) Piave, 8) Livenza, 9) Tagliamento, 10) Isonzo/Soča, 11) Timavo, 12) Rižana, 13) Dragonja, 14) Mirna, 15) Raša, 16) Bakarec and Rječina, 17) Dubračina and Senj HPP outflow, 18) Zrmanja, 19) Krka; b) locations of the ADCPs; c) subdivision by regions (I-IV); d) locations of the 5 selected sites.

provided vertical profiles of horizontal current speed for the following sites:

1. offshore Piran, Slovenia [45.55° N, 13.55° E: Malačič (2002)];
2. NE of the Po Delta, 14 km from Porto Viro, Italy (45.09° N, 12.59° E: courtesy of Adriatic LNG);
3. near Pašman (43.92° N, 15.33° E, reliable measured range from 6.1 to 56.1 m), Sedmovraće (44.20° N, 14.81° E, reliable measured range from 9.6 to 77.6 m), Pag (44.72° N, 14.73° E, reliable measured range from 9.9 to 81.9 m), and Grgur (44.89° N, 14.77° E, reliable measured range from 11.6 to 83.6 m), along the Croatian coast [courtesy of IOR: Vilibić *et al.* (2018)].

These instruments measure currents along the entire water column although, due to technical/design reasons (e.g. sidelobe interference, surface wave signals), the measurements within the topmost (of the order of some metres) layer are unreliable and were discarded (Malačič, personal communication).

Geostrophic currents were also estimated from average sea surface height satellite altimetric measurements (Pujol, 2021).

To summarise the results, validation assessment metrics root-mean-square differences

(*RMSD*s), biases and correlations (*C*) between models (*mod*) and observation (*obs*) have been computed [see Eq. (1)] for the current speed, and are presented in Tables 1, 2, and 3:

$$RMSD = \sqrt{(obs - mod)^2}$$
$$bias = obs - mod \qquad (1)$$
$$C = \frac{\langle obs \cdot mod \rangle - \langle obs \rangle \cdot \langle mod \rangle}{\sigma[obs]\sigma[mod]}.$$

Statistics for both the whole periods and seasons are shown.

3.4. The Betz Law

The maximum power flux (power per area unit of a surface perpendicular to the flow direction) that can be extracted from a moving fluid is not equal to the total kinetic power expressed by:

$$J = \frac{1}{2}\varrho v^3 \qquad (2)$$

with *v* being the flow speed and *ρ* the fluid density. From the conservation of mass and momentum, it can be shown (Betz, 1966) that this maximum power flux is given by:

$$J = \frac{8}{27}\varrho v^3 \qquad (3)$$

or by approximately 59% of the total.

Due to the non-linearity of this expression with regards to the flow speed, the average circulation is not sufficient to accurately describe the power available (e.g. $\langle J(v) \rangle \neq J\ (\langle v \rangle)$). Therefore, it is necessary to consider the full range of values of speed available and its distribution, in order to correctly estimate the power flux. Furthermore, we must point out that the NARF

Table 1 - Statistical metrics of current speed for VIDA buoy data.

		CMS - ADCP				**NARF – ADCP**			
		3 m		**19 m**		**3 m**		**19 m**	
RMSD [m/s]	JFM	0.052	0.056	0.038	0.037	0.049	0.055	0.039	0.040
	AMJ		0.042		0.047		0.043		0.038
	JAS		0.056		0.043		0.045		0.039
	OND		0.050		0.030		0.051		0.038
Bias [m/s]	JFM	0.036	0.043	0.023	0.021	-0.001	0.006	-0.008	-0.013
	AMJ		0.027		0.033		0.006		0.014
	JAS		0.035		0.028		0.000		-0.003
	OND		0.037		0.015		-0.009		-0.020
Correlation	JFM	-0.344	0.351	-0.427	0.687	-0.016	0.089	-0.510	0.685
	AMJ		-0.931		0.194		-0.571		0.139
	JAS		-0.491		0.184		0.141		0.312
	OND		0.182		0.488		-0.007		0.625

Table 2 - Statistical metrics of current speed for Porto Viro buoy data.

		CMS - ADCP				NARF – ADCP			
		3 m		26 m		3 m		26 m	
RMSD [m/s]	JFM	0.087	0.091	0.063	0.089	0.085	0.077	0.061	0.082
	AMJ		0.086		0.047		0.082		0.034
	JAS		0.097		0.050		0.092		0.041
	OND		0.069		0.055		0.088		0.073
Bias [m/s]	JFM	0.058	0.054	0.054	0.076	0.017	0.007	0.010	0.011
	AMJ		0.065		0.044		0.012		0.022
	JAS		0.082		0.044		0.048		0.018
	OND		0.027		0.049		-0.002		-0.011
Correlation	JFM	0.142	0.215	0.363	0.443	0.365	0.702	0.548	0.503
	AMJ		0.489		0.031		0.071		0.329
	JAS		0.441		0.251		0.001		0.284
	OND		-0.197		0.463		0.408		0.657

Table 3 - Statistical metrics of current speed for Croatian ADCPs; the CMS reanalysis resolution does not allow to discern the Pašman location from land, thus no values were available for a comparison.

		CMS - ADCP		NARF - ADCP	
		topmost	bottom	topmost	bottom
Pašman	RMSD [m/s]	/	/	0.106	0.047
	Bias [m/s]	/	/	0.071	0.037
	Correlation	/	/	0.152	0.095
Sedmovraće	RMSD [m/s]	0.096	0.034	0.078	0.030
	Bias [m/s]	0.079	0.024	0.024	0.013
	Correlation	0.061	0.034	0.094	0.161
Pag	RMSD [m/s]	0.083	0.051	0.061	0.034
	Bias [m/s]	0.074	0.041	0.033	0.015
	Correlation	0.233	0.172	0.034	0.388
Grgur	RMSD [m/s]	0.106	0.081	0.082	0.068
	Bias [m/s]	0.086	0.061	0.035	0.032
	Correlation	0.326	0.266	0.217	0.120

data set consists of daily averaged velocity outputs, signifying that higher frequency motions (e.g. tides) are filtered out.

3.5. Extreme value analysis

To better study velocity field variability, we performed a statistical analysis of the extreme values of speed. The analysis roughly follows the methodology outlined by Di Biagio *et al.* (2020) for the study of extreme event waves (EEWs) in the Mediterranean Sea. EEWs can be defined as contiguous regions in time and space that present values of a parameter of interest (e.g. chlorophyll concentrations or temperature - in the latter case they can be related to heat waves) higher than a given threshold, which could be either fixed *a priori* or be dependent on

the properties of the quantity itself (e.g. values over the 99th percentile). In our case, we are interested in current speed and, as a threshold, we chose the value of 0.6 m/s: for such a speed, in fact, the marine current power flux is comparable to, and even higher than, the wind power flux found in full-scale operational wind farms [for example in the Taranto offshore wind farm (https://renexia.it/en/beleolico-progetti/)].

The EEWs are identified as the ensemble of cells in a 3D (two spatial and one temporal dimensions) 'volume' with speed values higher than 0.6 m/s and connected along at least one side, either along the space or time dimension. Furthermore, we filtered out regions smaller than eight spatial cells and EEWs with duration shorter than two days, in order to avoid single-day spikes. With these settings, we obtained 37 events in the timespan of five years (2013-2017, see Section 4.2). To characterise each event, a number of specific indices can be computed, among which the following, specifically defined by Di Biagio *et al.* (2020):

- duration (T): the time interval, in days, from the first cell(s) to the last one(s);
- area (A): the total 2D spatial surface affected by the EEW;
- width (W): the total 3D volume of the EEW;
- uniformity (U): the ratio between width and volume of the prism bounding the EEW: $\frac{W}{AT}$, which represents a measure of EEW persistence;
- excess (E): the difference between the local value and threshold. In this specific case: $E(x, y, t) = |v(x, y, t)| - 0.6$ m/s.

We assessed the sensitivity of this method on the chosen threshold in speed by considering two other values, 0.5 and 0.7 m/s, and evaluated the average indices of duration, uniformity and excess together with the number of recorded EEWs.

4. Results

4.1. Model validation

4.1.1. Basin-scale comparison

Figs. 2a to 2d show the average seasonal (assuming that winter comprises January, February, and March, spring comprises April, May, and June, and so on) surface circulation reproduced by the NARF, which is found to be in qualitative agreement with literature sources. As shown in Poulain (2001), we observe an intensification of the WAC during autumn and winter months. Furthermore, we can recognise the formation of mesoscale structures [O (10 km) corresponding to local Rossby radius of deformation] in the summer months (July-August-September, JAS, Fig. 2c) due to the increased stratification caused by surface warming, while these patterns are absent due to the mixing occurring in the colder months (January-February-March, JFM, and October-November-December, OND, Figs. 2a and 2d).

A preliminary quality assessment of the NARF output can be performed by comparing the average surface circulation with the one obtained by satellite altimetric data and with surface currents produced by the CMS model, as shown in Figs. 3a to 3d. The four analyses represent some of the main circulation features, namely the WAC and the cyclonic gyre north of the Po Delta. However, we can readily notice an increase in the intensity of the currents and in the richness of dynamics and structures when moving from Figs. 3a to 3d.

Firstly, the average speed values are lower in the CMS products (both altimetric- and model-derived currents) with respect to the NARF ones. Indeed, we can infer from Fig. 3a that the circulation

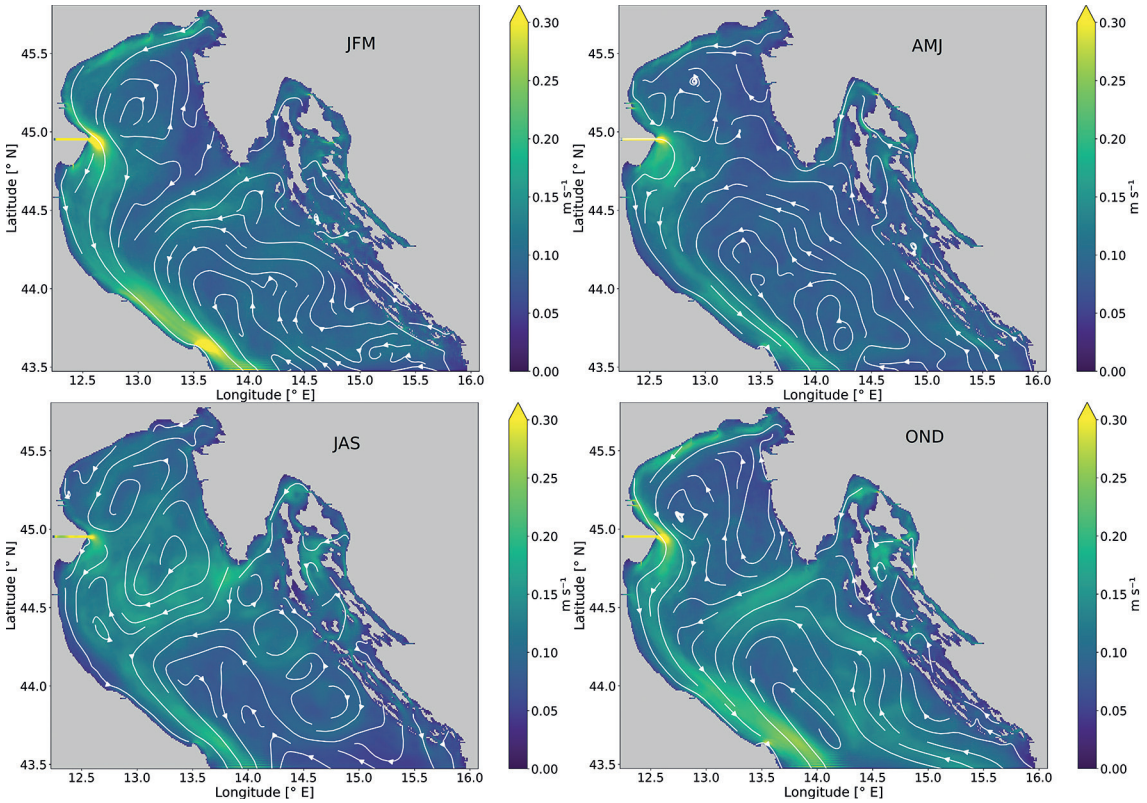

Fig. 2 - Average seasonal surface circulation from the NARF data set in winter (a: January-February-March), spring (b: April-May-June), summer (c: July-August-September), and autumn (d: October-November-December).

in the NAS has a strong a-geostrophic component. The circulation derived from the altimetric data only captures the main features (i.e. EAC entering and WAC exiting the basin, northern gyre) while it fails in describing the intensity of these currents. Moreover, since the Adriatic Sea is strongly affected by winds, the underestimation observed in the CMS reanalysis (Fig. 3b) can be ascribed to the low resolution (0.25° or 28 km) in the European Centre for Medium-Range Forecasts forcing, as demonstrated in the northern Adriatic basin by Denamiel *et al.* (2021): they showed strong discrepancies between a coarser ERA5 atmospheric model (with 30-kilometer resolution) and finer Weather Research and Forecasting implementations (with 3- and 1.5-kilometer resolution). The NARF model with the higher resolution shows a 50% increase in speed compared to the CMS currents. The impact of the atmospheric forcing is clear even within the same simulation, as shown in Figs. 3c and 3d. For the 2006-2012 period, the CADEAU service employed the RegCM model and, then, switched to the higher-resolution COSMO-I2 forcing. This change most likely affected surface dynamics: for example, a sharper turn of the currents that join the WAC from the open sea, the formation of meanders along the Dalmatian coast, and the presence of a second smaller anticyclonic gyre near the shores of the Istrian peninsula can be noticed.

4.1.2. Local comparisons

For a more quantitative evaluation, we can compare the models with the available in-situ observations, namely the ADCP measurements obtained by the VIDA buoy, the Porto Viro

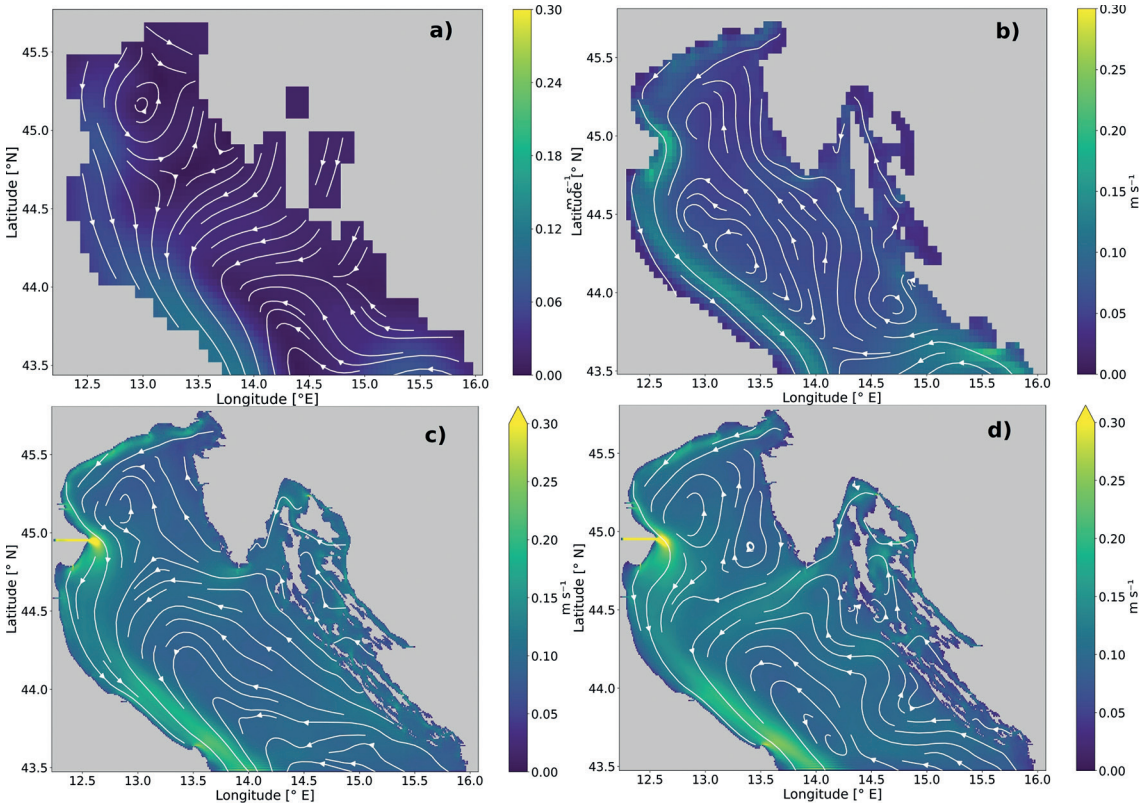

Fig. 3 - Comparison between surface average currents from: a) altimetric data; b) CMS reanalysis; c) NARF 2006-2012 simulation; d) NARF 2013-2017 simulation.

beacon and four instruments along the Croatian coast located near Pašman, Sedmovraće, Pag, and Grgur. We considered two levels of depth for each ADCP: the topmost and lowest depths available. As far as the VIDA buoy is concerned, the available data overlap the simulation for the years 2016 and 2017, while the Porto Viro measurements have been provided only from 2017 onwards. The Croatian ADCPs, instead, cover a period shorter than a year, from December 2014 to May (for the Sedmovraće instrument) or August 2015 (for the other three ADCPs).

Considering the metrics shown in Tables 1, 2, and 3, for all locations the bias obtained from the NARF-ADCP comparison is noticeably lower than the bias computed from the CMS reanalysis, indicating a closer agreement in average values of speed between the regional model and the observations. Conversely, the two models show similar, and relatively high, RMSDs, indicating low precision; in this case, the NARF captures the variability range of the measured data, but fails in precisely replicating the observed dynamics, as shown in the low values of correlation (0.5). The seasonal statistics for the Porto Viro measurements compared with the NARF data set show an intra-annual variability, with lower biases and higher correlations during winter and autumn months. This can be attributed to the more frequent episodes of Bora wind, which dominate basin dynamics by advecting surface waters along the Italian shoreline (e.g. at the Porto Viro buoy location), reducing the effects of other circulation patterns.

We also produced quantile-quantile (q-q) plots by comparing the distributions of the topmost ADCP speed measurements with the corresponding model layers from the CMS and NARF, as shown in Fig. 4. The plots compare the quantiles of the two data sets, with similarly distributed

data that fall close to the identity line (45° slope). From these plots we can further appreciate the improvement in the reproduced flow switching from the CMS reanalysis to the NARF system: while the former consistently underestimates the observed values, both at moderate speeds and for the outliers, the latter is in better agreement with the reference line, with more pronounced discrepancies at the higher speed values, which are more difficult to accurately reproduce.

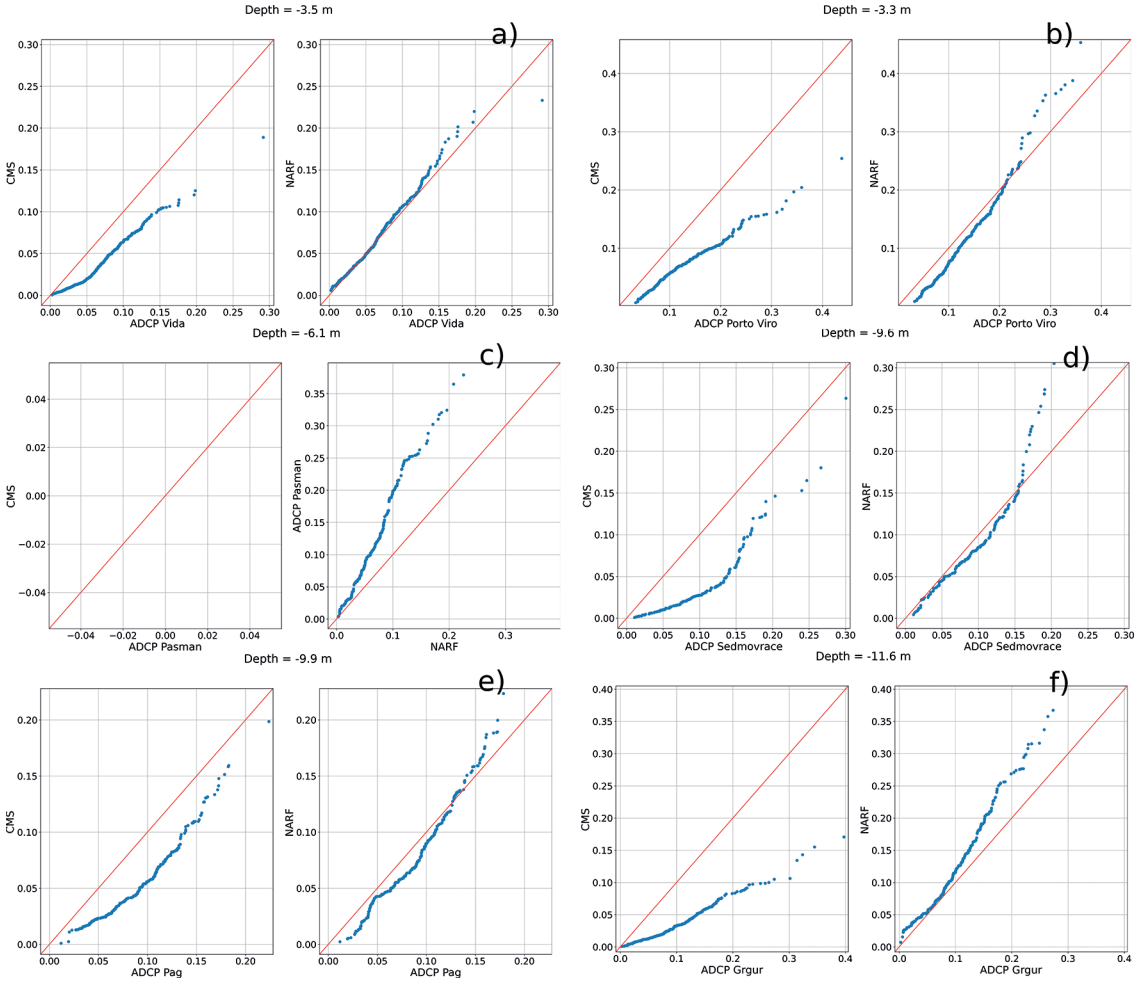

Fig. 4 - Q-q plots for the ADCP measurements compared with the CMS and NARF models; the CMS model resolution does not enable resolving the Pašman ADCP location (panel c), therefore a q-q plot could not be shown.

4.2. Application to marine energy assessment

Given the agreement (on average) with the observed speed values, we can employ the synthetic data set produced by the NARF to estimate the marine currents power in the NAS. We restricted the data timespan to the 2013-2017 simulated period, to more rigorously consider only the outputs produced by a single atmospheric forcing (i.e. higher-resolution COSMO), which already proved to reach stronger currents (Section 4.1.1.) and were satisfactorily compared with observations (Section 4.1.2.). We focused on the horizontal components of these currents, as the

vertical motions, despite their importance in the general circulation, carry a negligible fraction of the total kinetic energy: from the five-year NARF data set we obtain that the 95th percentile for the ratio of vertical/horizontal kinetic energy, $\frac{w^2}{u^2+v^2}$, is around 10^{-5}. Furthermore, for the marine energy assessment, we considered and averaged the flux over the first six NARF vertical levels, in the depth range from 0 to 20 m, in order to take into account the most energetic flows, as they are less affected by the bottom (no-slip boundary condition), as shown in the cross sections in Fig. 5.

4.2.1. Velocity and speed distribution

To study the distribution of the current speed we divided the NAS into four sub-regions, as shown in Fig. 1c, based on the main different bathymetric and circulation features:

I. area along the eastern Italian shores (approximately in front of the Emilia-Romagna and Marche regions) and with bathymetry shallower than 40 m;
II. area consisting of the northernmost part of the basin and including the regions in front of the lagoons of Venice and Grado-Marano, as well as the Gulf of Trieste, characterised by typical coastal dynamics and large freshwater input, and limited to a 40-metre depth;
III. waters between the rugged shoreline of Croatia and its islands, which can affect the circulation, and are characterised by steep gradients in bathymetry;
IV. the open sea region, less affected by coastal constraints and river contributions.

For this statistical analysis, we considered the surface layer of the NARF model (ranging from 0 to 1.5 m of depth) as it enables a better interpretation of the results: indeed, by averaging over the six topmost levels, some of the signals would be lost and the distributions, in particular for the horizontal components in the shallowest areas, would tend to shift towards lower values.

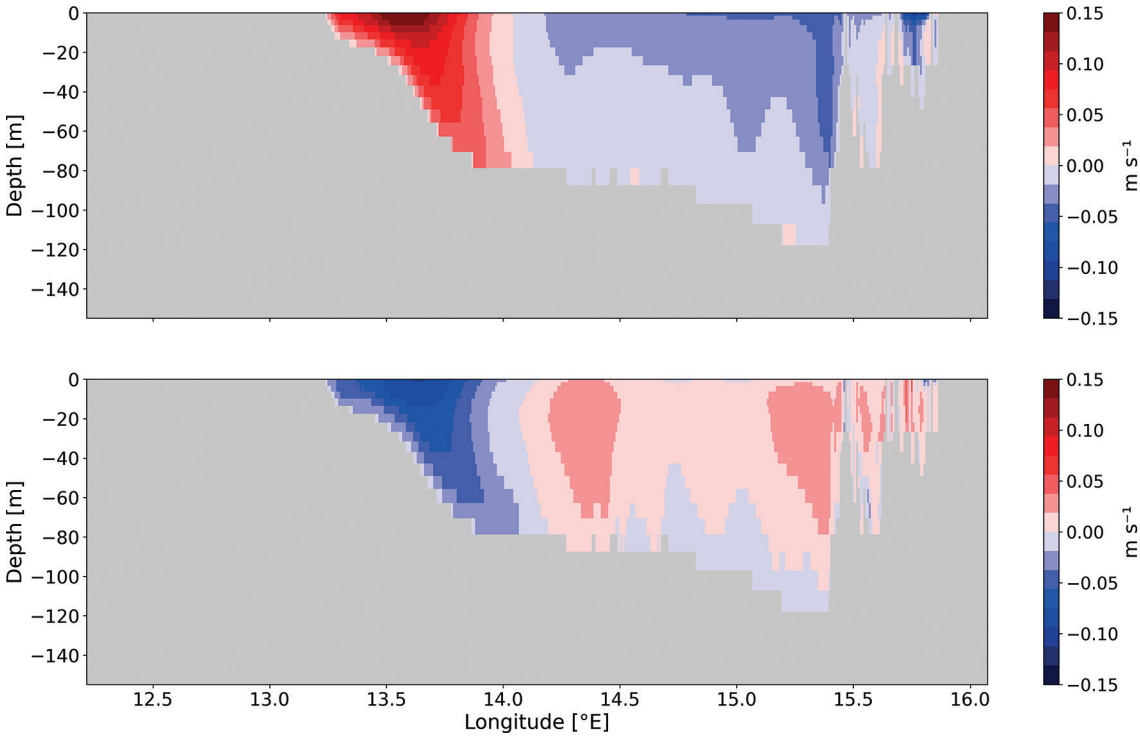

Fig. 5 - Cross sectional average zonal (upper) and meridional (lower) velocities for a 43.7°N transect.

The distributions are estimated via violin plots (Figs. 6 and 7), where the dashed lines represent the 25, 50 (median) and 75 percentiles. Each violin plot is computed by taking, as statistical sample, the whole time series of velocities (zonal and meridional components) or speed (magnitude) over each region and dividing by season, in order to discern the impact of the seasonal cycle.

Violin plots, cut at the 99.9th percentile, for the horizontal speed are shown in Figs. 6a to 6d. These plots highlight some interesting spatial differences: in particular, the distributions in region I are the ones with the highest values reached by both the tail and the median, always greater than 0.1 m/s. Moreover, Fig. 6a clearly displays the presence of a seasonal cycle, with the distributions 'stretching' in autumn and winter, with median values of 0.15 m/s, and 'squeezing' in spring and summer. This variability is consistent with the atmospheric conditions, as Bora events are more frequent during these months and can push waters, which are later advected into the WAC, westwards (Gačić and Artegiani, 2001).

We also produced violin plots for the current direction within the five years, as shown in Figs. 7a to 7d. In these plots, spread-out distributions can be observed in most of the sub-basins but in region I, where again the signal related to the WAC is clear, they can be observed with peaks centred around the SE direction, coherent with the direction of the outflowing current. In the other regions (II, III, and IV) we can observe signals that are caused by the general circulation patterns specific of the area. In region II, during autumn and winter, a WSW direction, compatible with flows due to Bora events, is noticeable and in region III the NW direction is dominant, in agreement with the inflow from the southern Adriatic. Instead, region IV shows a combination of the three previous signals, being an open sea area with less clear circulation patterns.

From these analyses, we can already identify a possible candidate for potential marine power applications in region I, as it is clearly the area that shows the highest values both in median speeds and in maximum values. To further analyse the distribution tails, focus is placed on the extremes in the following subsection.

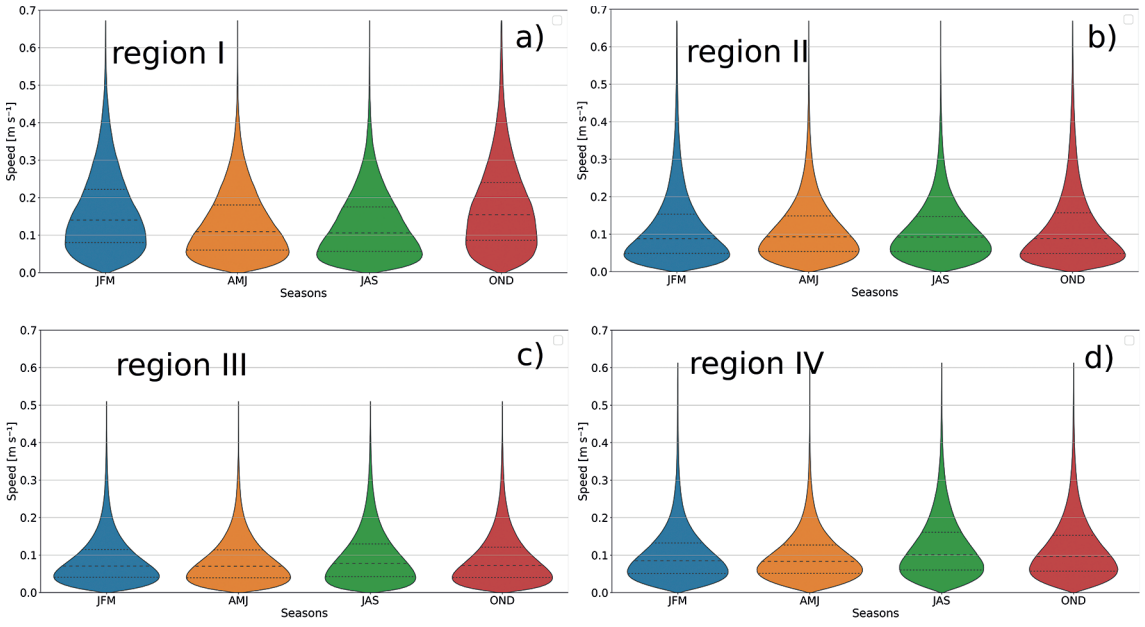

Fig. 6 - Seasonal violin plots of the four sub-basins for current speed.

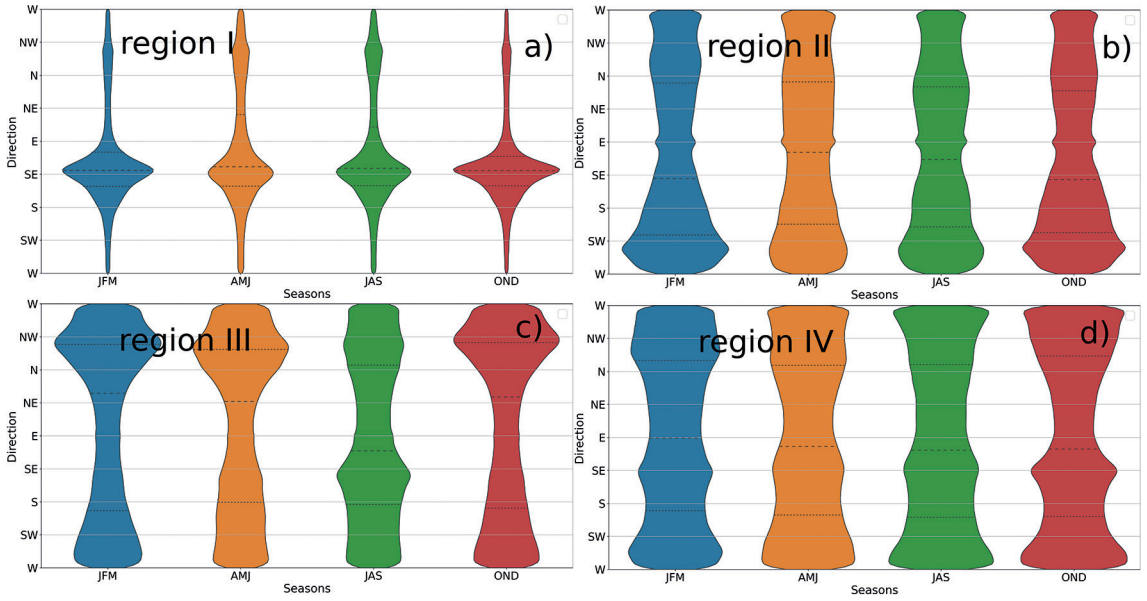

Fig. 7 - Seasonal violin plots of the four sub-basins for current direction.

4.2.2. Extreme value analysis

As described in Section 3.5, we compare the results derived from choices of different threshold values, shown in Fig. 8a: if we increase the threshold value we notice, as expected, a decrease in the number of EEWs (Fig. 8a-0) as well as in the duration and excess (Figs. 8a-1 and 8a-3), while the uniformity increases (Fig. 8a-1), due to EEWs being more limited in their spatio-temporal extension and, therefore, less variable. By averaging all the 37 EEWs, we obtain maps of the mean parameters, *T*, *U* and *E*, shown in Figs. 8b to 8d. The plots provide a synthetic view of the extreme values and their temporal and spatial properties (duration and persistence), useful in determining the impact of these events on the general circulation. These EEWs have durations (Fig. 8b) of a few days, up to a week at the most, as they are mainly driven by atmospheric forcing, with comparable time scales. For the uniformity index (Fig. 8c), we observe a higher average value in the open sea, specifically offshore southern Istria: these EEWs can be hypothesised to be more persistent as the Bora is more uniform when blowing over the open sea rather than near the coasts, where its flow is characterised by lee-side eddies and rotors (Grisogono and Belušić, 2009). The average excess (Fig. 8d) highlights the patterns already discussed, e.g. the strong currents flowing in front of the Po Delta, SE of Istria, and along the Italian coast (WAC).

4.2.3. Potential sites for ocean energy production

To identify the most promising sites, we summarise the information obtained from both average and extreme values, in order to better assess the available power. As far as EEWs are concerned, we selected the regions in which average duration *T* is at least three days, uniformity *U* larger than 0.3, and average excess *E* larger than 0.05 m/s, in order to filter out the less persistent and less intense average events.

Ultimately, we use the information regarding the average circulation to choose single sites (i.e. single model grid cells) from these regions by selecting the point with the highest mean

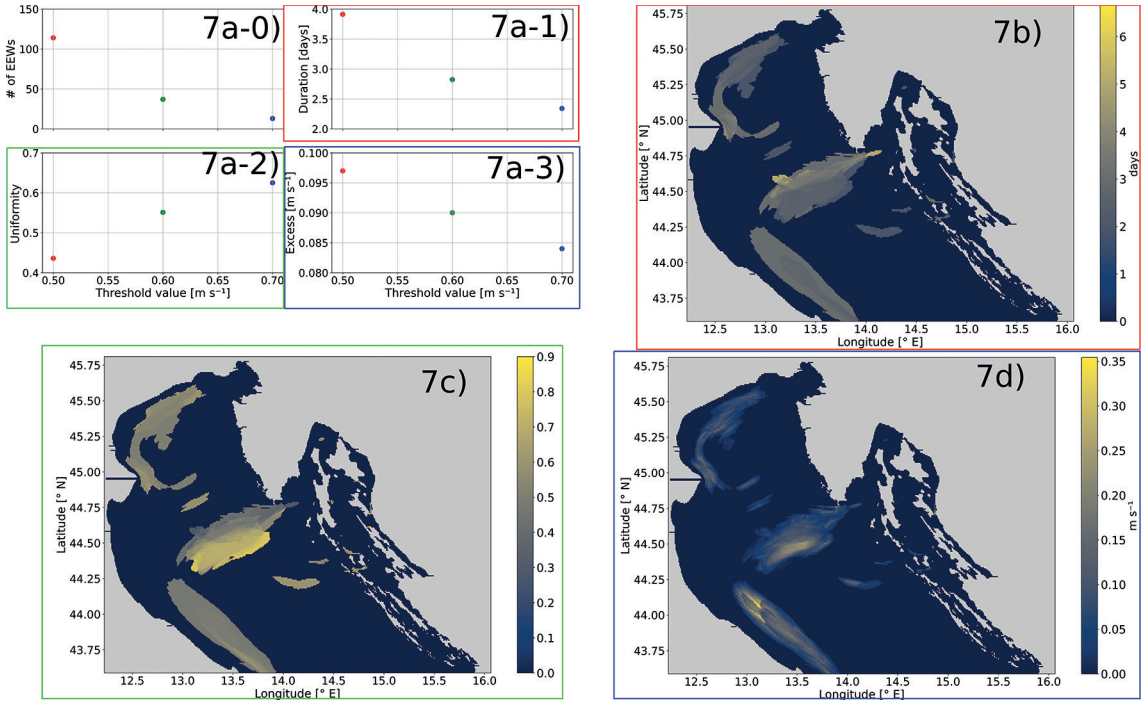

Fig. 8 - a) Sensitivity to different thresholds for EEW identification and their indices; b) average map of EEW duration; c) average map of EEW uniformity; d) average map of EEW excess.

speed. The chosen sites are:

- site Po (44.800° N, 12.696° E), model depth of 26.51 m;
- site Conero (43.548° N, 13.633° E), model depth of 26.51 m;
- site Krk (44.816° N, 14.758° E), model depth of 26.51 m;
- site Istria (44.612° N, 13.900° E), model depth of 21.84 m;
- site Rab (44.597° N, 14.870° E), model depth of 42.68 m.

Although an EEW region is absent for the last site, in light of the average values, this area proves to be favourable for energy production purposes and is also geographically similar (i.e. inlet between island and mainland) to the Krk-Prvić site.

For each site, as shown in Fig. 1d, the corresponding time series for the 0-17.5-metre layer-averaged speed was extracted from the NARF data set and, then, the available power flux was calculated by applying the Betz Law [as shown in Eq. (2)], considering a constant density of ρ = 1,028 kg/m³. While we know that the northern Adriatic is characterised by strong density variability induced by large freshwater inputs, intense evaporation, and deep-water formation (Cushman-Roisin *et al.*, 2001), we can neglect these variations as they are at most of the order of some permille and further outweighed by the cubic dependence of power with speed [Eq. (3)].

To better visualise the different properties of the selected sites, we computed the duration curves for the power flux, as shown in Fig. 9, simulated by using the higher-resolution atmospheric model. These curves are obtained by sorting the time series in speed decreasing order, and indicate, for a given value of power flux on the x-axis, the number of days over the whole time period, normalised with its duration, when power is higher than that specific value. This curve represents the complementary cumulative distribution of power flux.

All the curves show, for around 50% of the time, low values of available power (< 1 W/m²).

The difference in power for each site is, instead, usually due to the tails of these curves, with Po and Krk showing the most extended ones.

5. Discussion on power generation feasibility

Among the five proposed locations, the most interesting site, in terms of available power, is the strait between the islands of Krk and Prvić in Croatia. As shown in Fig. 9, an average power flux of 10.3 W/m² is reached when considering the five-year period (from 2013 to 2017) of the simulation. It is important to highlight, however, that this site is represented in the model discretisation by a single grid point between two islands, which, therefore, may impose resolution-dependent topographic constraints on the simulated flow: an open question concerns how reliable the results of this simulation, for these peculiar bathymetric conditions, are.

Noteworthy is how the results of the analysis for current speed do not drastically change if the whole 12-year simulation is considered, with averages, for example, varying from 5 to 10%, with the most noticeable fluctuations in very coastal regions, such as the Krk-Prvić site, where they reach around 20% differences. Conversely, the change in the estimated power density is relevant: the Krk-Prvić site, for example, shows an average power flux, over the 2006-2017 time period, of approximately 5.8 against the 10.3 W/m² estimated only with the 2013-2017 simulated period.

Considering the results obtained, no sites or regions are suitable for large-scale energy production: the power fluxes in the five sites analysed are much lower (of about one order of magnitude) than the typical offshore wind farms, here chosen as reference. Even for the Krk-Prvić site, the average power flux of ~10 W/m² is significantly lower than the ~65 W/m² obtained for the Taranto offshore wind farm.

The difference is even more pronounced when compared with other possible sites of ocean energy production in the Mediterranean Sea. The Strait of Messina is one of the most promising locations for marine current power generation (Coiro and Troise, 2012): the energy content in this site is estimated by using the CMS reanalysis over the 2013-2017 time period. As seen in Section 3, CMS products usually underestimate current speed, hence, the following estimate can be

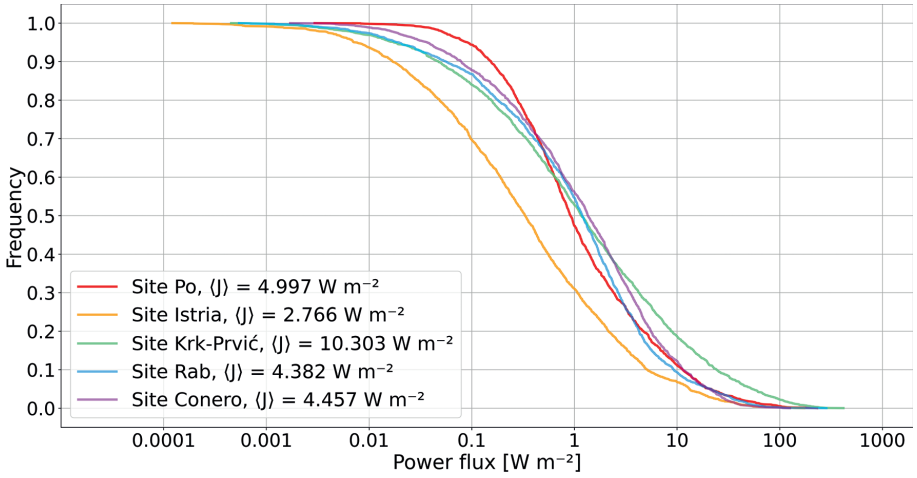

Fig. 9 - Duration curves for the different sites in the 2013-2017 period.

considered conservative. As seen in Fig. 10, the average power flux in the Strait ($\langle J \rangle$ = 135.9 W/m²) is much higher than that of the NAS sites, and it also doubles the value obtained for the Taranto wind farm. This large difference is due to the strong currents that characterise the Strait of Messina. It is very important to also notice that the CMS reanalysis provides only daily averaged values, hence, the very strong tidal signal in the Strait (Coiro and Troise, 2012) is neglected. Therefore, the computation of power flux in this paper is most likely strongly underestimated. Furthermore, we also plot the power curves for a CMS reanalysis grid point offshore Ancona, approximately corresponding to the Conero site, in order to show the impact of our higher-resolution model on the power flux estimate. When compared to the CMS 'Ancona' site, the NARF Conero one shows three times higher marine current power. It is, thus, reasonable that a high-resolution model simulating an area including the Strait of Messina, with high frequency output (resolving tides), could lead to a noticeable increase in the estimated power fluxes.

From the validation performed in Section 4, we noticed a good agreement with the considered observations. Therefore, the power flux computed by current measurements is not expected to be much higher than our model estimates, even though more observations would be required to verify or disprove this hypothesis. However, it is important to note that, as seen in Section 4, a small increase in average speed can lead to significant gain in available power; in particular, to achieve power fluxes of 65 W/m² it would be necessary to have average currents around 0.48 m/s that, albeit still higher than the ones reproduced by the model, are not completely out of range for intense currents in the Mediterranean and even in the Adriatic Sea (Janeković *et al.*, 2020).

Nonetheless, potential interest could arise for small scale electricity generation, where some units (turbines) could power infrastructures with a low energy demand, particularly by employing specific design solutions, such as ducted and/or open centre turbines (Belloni, 2013). In the case of ducted turbines, these can achieve higher power density over the area swept by the blades by converging the incoming flow at the entrance of the duct (whose area is wider than that of the turbine), at the cost of a larger cross-sectional surface required per device. For low demand applications, however, the number of turbines needed would be lower and, hence, the constraint on the design of the turbines array would be less restrictive. An example of these small-scale applications could be in the field of aquaculture (e.g. fish and mussel farming for

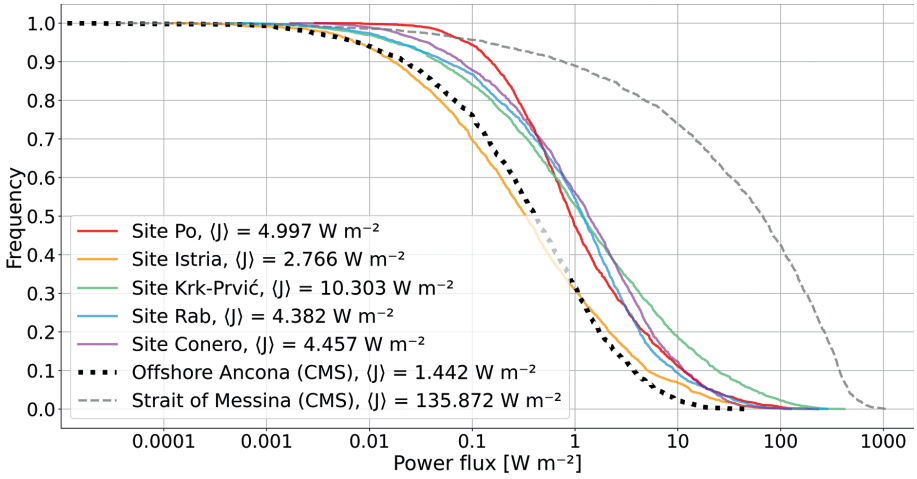

Fig. 10 - Duration curves compared with estimates from CMS reanalysis in the 2013-2017 period.

human consumption). Some of these installations need power for their operational functioning, for example, for feeding and monitoring of environmental parameters, which could be provided by in-situ energy sources (Ley, 2022), such as marine currents. These environmental sensors need electricity supplies of the order of 0.1÷10 W per unit (https://aquamonitrix.com/), so that a single small turbine, with a few metres in diameter (Coiro *et al.*, 2009), could power more than one instrument. Indeed, one of the objectives of the Sustainable Blue Economy outlined by the European Commission (European Commission, 2021) is to expand the scope of sustainable ocean exploitation also through the integration and cooperation of different sectors, such as aquaculture and renewable energy.

As a matter of fact, the Adriatic is an important productive area in the field of aquaculture, with many installations already operational, while also hosting various biologically significant areas, as shown in Fig. 11 [from the HarmoNIA GeoPortal on Vulnerability of coastal areas (https://vrtlac.izor.hr/harmonia/index.html)]. The presence of many farms can be observed along the coasts of Croatia and Italy and, in the latter case, many of these can be found in regions here identified as some of the most interesting in terms of available power: the Po Delta and the Emilia-Romagna and Marche coastal areas.

On the other hand, the presence of other human activities, such as fisheries and maritime traffic routes, and of marine habitats, could limit the choice of potential sites. As shown in Fig. 11, the northern Adriatic hosts many marine protected areas and other sites of ecological relevance. In particular, protected areas and biologic protection zones are indicated: both function as

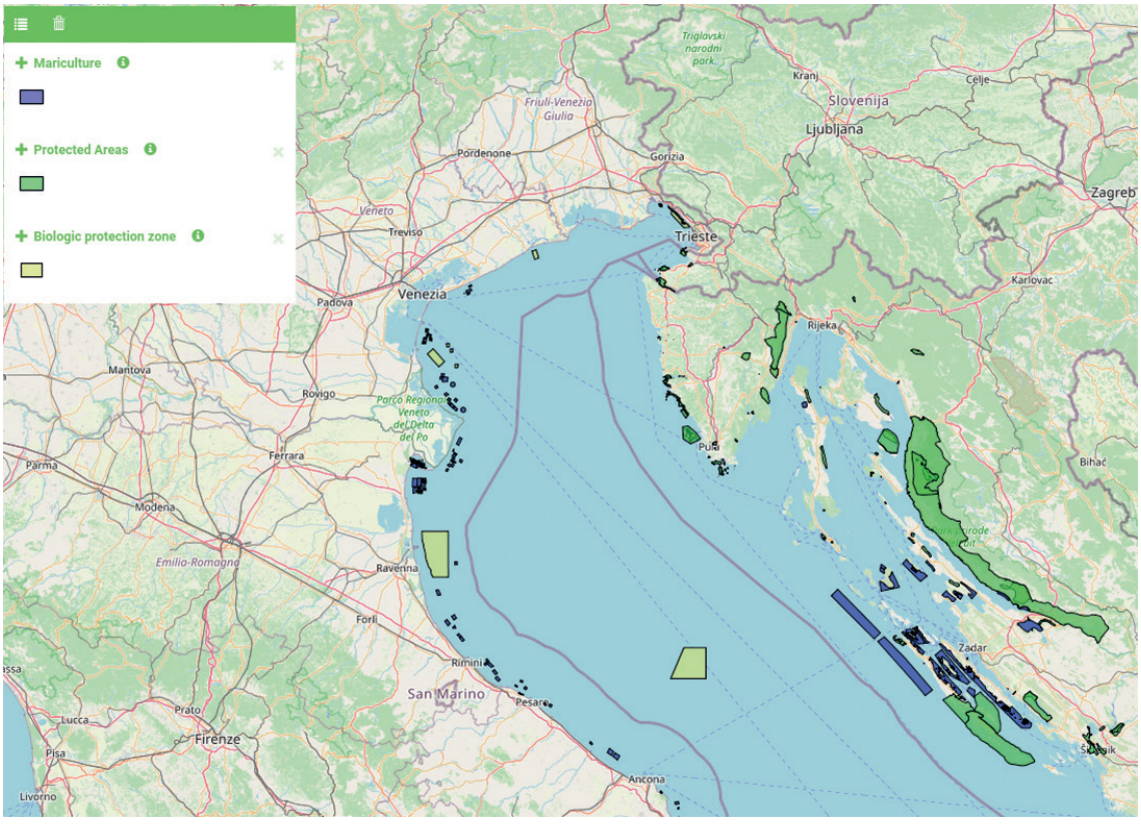

Fig. 11 - Location of protected areas (darker shade of green), biologic protection zones (lighter shade of green) and aquaculture installations (blue) in the northern Adriatic (from the HarmoNIA GeoPortal).

conservation areas for ecologically important habitats, but with varying degrees of limitations on human activities (from fishing and maritime traffic to recreational bathing).

To this concern, the Tethys database (https://tethys.pnnl.gov/) provides data to support studies and research regarding the environmental effects of marine renewable energies, from offshore wind to wave and marine currents. Among the possible impacts of generic power generation infrastructures, marine turbines mainly cause risks of collision with moving parts (turbine blades) and the generation of underwater noise and electromagnetic fields, which can affect specific sensitive animals. From the most recent studies reported by the Tethys project, collision alone seems to represent a relevant risk to marine fauna, requiring, thus, a proper planning in order not to impact these organisms, in particular those belonging to species already under multiple stressors (overfishing, pollution, etc.).

As regards the technological and engineering aspects, in the actual power output evaluation, it must be taken into account that the Betz Power Coefficient (C_p) is the maximum theoretical limit. Actual C_p is expected to be lower.

By noticing that the typical efficiency of Kaplan hydraulic turbines is between 90 ÷ 95% (Dixon and Hall, 2010) and that, in this case, the ideal limit could be identified as 100% (without friction losses and with a full kinetic energy recovery in the draft tube), the actual C_p for non-ducted turbines may be evaluated at approximately 90% of the Betz limit. For ducted turbines, the Betz limit could, in principle, be exceeded and an accurate fluid dynamic analysis would be required to evaluate the expected actual C_p (Belloni *et al.*, 2017).

6. Conclusions

The present work provides an analysis of the circulation features in the NAS on a basin scale. The NARF, a high-resolution modelling system (1/128° resolution horizontal grid), was firstly validated against *in-situ* current measurements, showing a good agreement in terms of expected values and ranges of variability (Tables 1 and 2): in particular, the NARF data set reports a noticeably lower bias with respect to the lower resolution CMS reanalysis.

Subsequently, the horizontal currents simulated by the system over a five-year period (2013-2017) were analysed. Focus was placed on the extreme values of velocity, estimating the speed distributions and their tails in four sub-basins, defined on a dynamical and bathymetric basis. We found the highest and most temporally stable speeds in region I, which follows the Italian shore south of the Po Delta.

In analogy with heatwaves, EEWs were also identified. We found 37 EEWs characterised by a temporal duration of a few days (approximately three, on average) but also by high values of current speed.

From these analyses, we, first, sought the most promising regions, and, then, locations, for potential power generation from marine currents: by integrating the information about the average circulation and these extreme values, the five final sites were identified. While none of these were found to be suitable for large scale energy production, the power flux (computed by applying the Betz Law) showed a major increase if estimated with the NARF rather than lower-resolution simulations, up to three times in some locations. The results obtained highlight the important role of speed distribution tails and, therefore, of sufficiently detailed simulations to reproduce these extremes.

The synthetic data set obtained from the NARF simulation consisted of daily averages. A more temporally refined data set (for example, with hourly averages) could further update,

realistically increasing, the estimates obtained in this work, allowing, for example, the evaluation of potentially important contributions due to tidal motions.

Another further development could envisage the extension and porting of the methods developed in this study to other basins, simulated with high resolution modelling tools. During the SHAREMED project (https://sharemed.interreg-med.eu/), for example, the NARF system has been relocated to different regions of the Mediterranean Sea (i.e. the Strait of Sicily, Ligurian Sea, Gulf of Lion, and Catalan Sea), thus potentially offering the opportunity to perform similar analyses in those areas.

Acknowledgments. The authors thank Vlado Malačič and the Slovenian National Institute of Biology (http://www.nib.si/) for the fruitful discussion and exchanges regarding the functioning of the VIDA oceanographic buoy and interpretation of the ADCP data. We thank Adriatic LNG (https://www.adriaticlng.it/) for providing the data obtained offshore Porto Viro. We are also grateful to the Institute of Oceanography and Fisheries (www.izor.hr) for kindly providing the ADCP data collected in the framework of the North Adriatic Dense Water Experiment 2015 (NAdEx 2015), which gave useful insight into more coastal locations along the Croatian shoreline. This study was conducted using EU Copernicus Marine Service information. This study was carried out in the framework of the project iNEST – Interconnected Nord-Est Innovation Ecosystem, funded by the European Union – NextGenerationEU (ECS00000043 – CUP J43C22000320006).

REFERENCES

Adcroft A., Campin J.-M., Doddridge E., Dutkiewicz S., Evangelinos C., Ferreira D., Follows M., Forget G., Fox-Kemper B., Heimbach P., Hill C., Hill E., Hill H., Jahn O., Klymak Losch M., Marshall J., Maze G., Mazloff M., Menemenlis D., Molod A. and Scott J.; 2022. *MITgcm Documentation.* https://doi.org/https://doi.org/10.5281/zenodo.1409237

Belloni C.; 2013: *Hydrodynamics of ducted and open-centre tidal turbines.* PH.D. Thesis in Phylosophy, University of Oxford, Oxford, UK, 240 pp.

Belloni C.S.K., Willden R.H.J. and Houlsby G.T.; 2017: *An investigation of ducted and open-centre tidal turbines employing CFD-embedded BEM*. Renewable Energy, 108, 622-634.

Betz A.; 1966: *Introduction to the Theory of Flow Machines*. Pergamon Press, Oxford, UK, 281 pp.

Brito-Melo A., Bhuyan G., Nielsen K., Polaski K., Pontes T. and Shanahan G.; 2007. *Ocean energy systems implementing agreement: an international collaborative programme.* Proc. 16th International Offshore and Polar Engineering Conference, Lisbon, Portugal, p. 463.

Bruschi A., Lisi I., De Angelis R., Querin S., Cossarini G., Di Biagio V. and Silvestri C.; 2021: *Indexes for the assessment of bacterial pollution in bathing waters from point sources: the northern Adriatic Sea CADEAU service*. J. Environ. Manage., 293, 112878, 14 pp.

Calero Quesada M.C., García Lafuente J., Sánchez Garrido J.C., Sammartino S. and Delgado J.; 2014: *Energy of marine currents in the Strait of Gibraltar and its potential as a renewable energy resource.* Renewable Sustainable Energy Rev., 34, 98-109, doi: 10.1016/j.rser.2014.02.038.

Coiro D. and Troise G.; 2012: *Stima della produzione energetica da correnti marine nello Stretto di Messina.* ENEA, Roma, Italy, Report RdS/2012/172, 52 pp.

Coiro D., De Marco A., Scherillo F., Maisto U., Familio R. and Troise G.; 2009: *Harnessing marine current energy with tethered submerged systems: experimental tests and numerical model analysis of an innovative concept.* In: Proc. International Conference on Clean Electrical Power, Capri, Italy, pp. 76-86, doi: 10.1109/ICCEP.2009.5212080.

Coiro D., Troise G. and Bizzarrini N.; 2018: *Experiences in developing tidal current and wave energy devices for Mediterranean Sea*. Front. Energy Res., 6, 136, 16 pp., doi: 10.3389/fenrg.2018.00136.

Cossarini G., Querin S. and Solidoro C.; 2015: *The continental shelf carbon pump in the northern Adriatic Sea (Mediterranean Sea): influence of wintertime variability*. Ecol. Modell., 314, 118-134, doi: 10.1016/j.ecolmodel.2015.07.024.

Cossarini G., Querin S., Solidoro C., Sannino G., Lazzari P., Di Biagio V. and Bolzon G.; 2017: *Development of BFMCOUPLER (v1.0), the coupling scheme that links the MITgcm and BFM models for ocean biogeochemistry simulations.* Geosci. Model Dev., 10, 1423-1445, doi: 10.5194/gmd-10-1423-2017, 2017.

Cushman-Roisin B., Gačić M., Poulain P.-M. and Artegiani A.; 2001: *Physical Oceanography of the Adriatic Sea: past, present and future, ed. 1*. Springer, Dordrecht, Germany, 320 pp., doi: 10.1007/978-94-015-9819-4.

Denamiel C., Pranić P., Quentin F., Mihanović H. and Vilibić I.; 2020: *Pseudo-global warming projections of extreme wave storms in complex coastal regions: the case of the Adriatic Sea*. Clim. Dyn., 55, 2483-2509, doi: 10.1007/s00382-020-05397-x.

Denamiel C. , Tojčić I. and Vilibić I.; 2021. *Balancing accuracy and efficiency of atmospheric models in the northern Adriatic during severe bora events.* Journal of Geophysical Research: Atmospheres, 126, e2020JD033516. https://doi.org/10.1029/2020JD033516.

Di Biagio V., Cossarini G., Salon S. and Solidoro C.; 2020: *Extreme event waves in marine ecosystems: an application to Mediterranean Sea surface chlorophyll*. Biogeosci., 17, 5967-5988, doi: 10.5194/bg-17-5967-2020.

Dixon S.L. and Hall C.A.; 2010: *Fluid mechanics and thermodynamics of turbomachinery, 6th ed.* Elsevier Inc., Burlington, MA, USA, 469 pp.

Escudier R., Clementi E., Omar M., Cipollone A., Pistoia J., Aydogdu A., Drudi M., Grandi A., Lyubartsev V., Lecci R., Cretí S., Masina S., Coppini G. and Pinardi N.; 2020: *Mediterranean Sea physical reanalysis (CMEMS MED-Currents) (Version 1) data set*. Copernicus Monitoring Environment Marine Service (CMEMS), doi: 10.25423/CMCC/MEDSEA_MULTIYEAR_PHY_006_004_E3R1.

Escudier R., Clementi E., Cipollone A., Pistoia J., Drudi M., Grandi A., Lyubartsev V., Lecci R., Aydogdu A., Delrosso D., Omar M., Masina S., Coppini G. and Pinardi N.; 2021: *A high resolution reanalysis for the Mediterranean Sea*. Front. Earth Sci., 9, 702285, 20 pp., doi: 10.3389/feart.2021.702285.

European Commission; 1996: *The exploitation of tidal and marine currents: Non-nuclear Energy JOULE II; Wave energy project results.* Publications Office of the European Communities, Luxembourg, 65 pp.

European Commission; 2021: *On a new approach for a sustainable blue economy in the EU Transforming the EU's Blue Economy for a Sustainable Future.* Publications Office of the European Communities, Luxembourg, 21 pp.

Ferrarin C., Valentini A., Vodopivec M., Klaric D., Massaro G., Bajo M., De Pascalis F., Fadini A., Ghezzo M., Menegon S., Bressan L., Unguendoli S., Fettich A., Jerman J., Ličer M., Fustar L., Papa A. and Carraro E.; 2020: *Integrated seastorm management strategy: the 29 October 2018 event in the Adriatic Sea.* Nat. Hazards Earth Syst. Sci., 20, 73-93, doi: 10.5194/nhess-20-73-2020.

Gačić M. and Artegiani A.; 2001: *Regional studies: Italian coastal waters.* In: Cushman-Roisin B., Gačić M., Poulain P.-M. and Artegiani A.; 2001: Physical Oceanography of the Adriatic Sea: past, present and future, ed. 1. Springer, Dordrecht, Germany, pp. 182-189.

Gačić M., Poulain P.-M., Zore-Armanda M. and Barale V.; 2001: *Overview.* In: Cushman-Roisin B., Gačić M., Poulain P.-M. and Artegiani A.; 2001: Physical Oceanography of the Adriatic Sea: past, present and future, ed. 1. Springer, Dordrecht, Germany, pp. 1-44.

Giorgi F., Coppola E., Solmon F., Mariotti L., Sylla M.B., Bi X., Elguindi N., Diro G.T., Nair V., Giuliani G., Turuncoglu U.U., Cozzini S., Güttler I., O'Brien T.A., Tawfik A.B., Shalaby A., Zakey A.S., Steiner A.L., Stordal F., Sloan L.C. and Brankovic C.; 2012: *RegCM4: model description and preliminary tests over multiple CORDEX domains*. Clim. Res., 52, 7-29, doi: 10.3354/cr01018.

Grisogono B. and Belušić D.; 2009: *A review of recent advances in understanding the meso- and microscale properties of the severe Bora wind*. Tellus Ser. A: Dyn. Meteorol. Oceanogr., 61, 1-16, doi: 10.1111/j.1600-0870.2008.00369.x.

Hadžić N., Kozmar H. and Tomić M.; 2014: *Offshore renewable energy in the Adriatic Sea with respect to the Croatian 2020 energy strategy.* Renewable Sustainable Energy Rev., 40, 597-607, doi: 10.1016/j.rser.2014.07.196.

Hazim S., Salih A., Taha Janan M., Ouatouati A.E. and Ghennioui A.; 2021: *Marine current energy assessment and the hydrodynamic design of the hydrokinetic turbine for the Moroccan Mediterranean coast.* Energy Explor. Exploit., 39, 717-737, doi: 10.1177/0144598720986629.

Janeković I., Mihanović H., Vilibić I., Grčić B., Ivatek-Šahdan S., Tudor M. and Djakovac T.; 2020: *Using multi-platform 4D-Var data assimilation to improve modeling of Adriatic Sea dynamics*. Ocean Modell., 146, 101538, doi: 10.1016/j.ocemod.2019.101538.

Kuzmić M., Janeković I., Book J.W., Martin P.J. and Doyle J.D.; 2006: *Modeling the northern Adriatic double-gyre response to intense bora wind: a revisit*. J. Geophys. Res., 112, C03S13, 27 pp., doi: 10.1029/2005JC003377.

Ley C.; 2022: *Partnership potential: wave energy firms see the benefits of working with the aquaculture sector.* Fish Farmer Mag., 45, 44-45.

Ličer M., Smerkol P., Fettich A., Ravdas M., Papapostolou A., Mantziafou A., Strajnar B., Cedilnik J., Jeromel M., Jerman J., Petan S., Malačič V. and Sofianos S.; 2016: *Modeling ocean response to an extreme Bora event in northern Adriatic using one-way and two-way atmosphere-ocean coupling.* Ocean Sci., 12, 71-86, doi: 10.5194/os-12-71-2016.

Lipizer, M., Partescano, E., Rabitti, A., Giorgetti, A., and Crise, A.; 2014: *Qualified temperature, salinity and dissolved oxygen climatologies in a changing Adriatic Sea*, Ocean Sci., 10, 771-797, https://doi.org/10.5194/os-10-771-2014.

Malačič V.; 2002: *Technical description of coastal oceanographic buoy* (tech. Rep.). Available at https://www.nib.si/mbp/en/oceanographic-data-and-measurements/buoy-2/documentation-2 (URL last visited on 26/07/2024).

Nikolaidis N., Karaolia A., Matsikaris A., Nikolaidis A., Nicolaides M. and Georgiou G.C.; 2019: *Blue energy potential analysis in the Mediterranean.* Front. Energy Res., 7, 1-12, doi: 10.3389/fenrg.2019.00062.

Petronio A., Roman F., Nasello C. and Armenio V.; 2013: *Large eddy simulation model for wind-driven sea circulation in coastal areas*. Nonlinear Processes Geophys., 20, 1095-1112, doi: 10.5194/npg-20-1095-2013.

Poulain P.-M.; 2001: *Adriatic Sea surface circulation as derived from drifter data between 1990 and 1999*. J. Mar. Syst., 29, 3-32, doi: 10.1016/S0924-7963(01)00007-0.

Poulain P.-M. and Cushman-Roisin B.; 2001: *Circulation.* In: Cushman-Roisin B., Gačić M., Poulain P.-M. and Artegiani A.; 2001: Physical Oceanography of the Adriatic Sea: past, present and future, ed. 1. Springer, Dordrecht, Germany, pp. 67-109.

Poulain P.-M. and Raicich F.; 2001: *Forcings.* In: Cushman-Roisin B., Gačić M., Poulain P.-M. and Artegiani A.; 2001: Physical Oceanography of the Adriatic Sea: past, present and future, ed. 1. Springer, Dordrecht, Germany, pp. 45-65.

Pranić P., Denamiel C. and Vilibić I.; 2021: *Performance of the Adriatic Sea and Coast (AdriSC) climate component - a COAWST V3.3-based one-way coupled atmosphere-ocean modelling suite: ocean results*. Geosci. Model Dev., 14, 5927-5955, < gmd.copernicus.org/articles/14/5927/2021/ >.

Pujol M.-I.; 2021: *Product user manual for sea level SLA products.* Copernicus marine environment monitoring service. Tech. Rep., 51 pp.

Querin S., Cossarini G. and Solidoro C.; 2013: *Simulating the formation and fate of dense water in a mid-latitude marginal sea during normal and warm winter conditions*. J. Geophys. Res.: Oceans, 118, 885-900, doi: 10.1002/jgrc.20092.

Querin S., Bensi M., Cardin V., Solidoro C., Bacer S., Mariotti L., Stel F. and Malačič V.; 2016: *Saw-tooth modulation of the deep-water thermohaline properties in the southern Adriatic Sea*. J. Geophys. Res.: Oceans, 121, 4585-4600, doi: 10.1002/2015JC011522.

Querin S., Cosoli S., Gerin R., Laurent C., Malačič V., Pristov N. and Poulain P.-M.; 2021: *Multi-platform, high-resolution study of a complex coastal system: the TOSCA experiment in the Gulf of Trieste*. J. Mar. Sci. Eng., 9, 469, 28 pp., doi: 10.3390/jmse9050469.

Silvestri C., Bruschi A., Calace N., Cossarini G., De Angelis R., Di Biagio V., Giua N., Peleggi M., Querin S., Saccomandi F., Salon S., Solidoro C. and Spada E.; 2020: *CADEAU project - final report.* National Institute for Oceanography and Applied Geophysics, 34 pp., doi: 10.6084/m9.figshare.12666905.v1.

Solidoro C., Bastianini M., Bandelj V., Codermatz R., Cossarini G., Melaku Canu D., Ravagnan E., Salon S. and Trevisani S.; 2009, *Current state, scales of variability, and trends of biogeochemical properties in the northern Adriatic Sea*, J. Geophys. Res., 114, C07S91, doi: "https://doi.org/10.1029/2008JC004838"10.1029/2008JC004838.

Umgiesser G., Ferrarin C., Bajo M., Bellafiore D., Cucco A., De Pascalis F., Ghezzo M., McKiver W., Arpaia L.; 2022: *Hydrodynamic modelling in marginal and coastal seas - The case of the Adriatic Sea as a permanent laboratory for numerical approach*. Ocean Model., 179, 102123, doi: 10.1016/j.ocemod.2022.102123.

Vichi M., Lovato T., Lazzari P., Cossarini G., Gutierrez Mlot E., Mattia G., Masina S., McKiver W.J., Pinardi N., Solidoro C., Tedesco L. and Zavatarelli M.; 2015: *The Biogeochemical Flux Model (BFM): equation description and user manual*. *BFM version 5.1*. BFM Consortium, Bologna, Italy, 104 pp., < bfm-community.eu >.

Vilibić I., Mihanović H., Janeković I., Denamiel C., Poulain P.-M., Orlić M., Dunić N., Dadić V., Pasarić M., Muslim S., Gerin R., Matić F., Šepić J., Mauri E., Kokkini Z., Tudor M., Kovač Ž. and Džoić T.; 2018: *Wintertime dynamics in the coastal northeastern Adriatic Sea: the NAdEx 2015 experiment.* Ocean Sci., 14, 237-258, doi: 10.5194/os-14-237-2018.

Corresponding author: Fabio Giordano
National Institute of Oceanography and Applied Geophysics
Via Beirut 2, 34151 Trieste, Italy
Phone: +39-040-2140-649; e-mail: fgiordano@ogs.it